Study of polarization effects on distributed vibration sensing based on FBGs array

Fourier Sandah[1,2], Michel Dossou[2], Marc Wuilpart[1]

[1]Electromagnetism and Telecommunications Department, University of Mons, Mons, Belgium
[2]University of Abomey-Calavi, URPHORAN, Polytech School of Abomey-Calavi, LETIA, Cotonou, Benin

Structural health monitoring has recently attracted much attention in research and development thanks to distributed optical fibre sensors. Among distributed optical fibre sensors, phase-sensitive optical time-domain reflectometry (φ-OTDR) allows distributed vibration sensing by analysing the interference properties of the backscattered/reflected signal when an optical pulse is launched into the sensing fibre[1]. As the Rayleigh backscattered light is relatively weak, fibre Bragg grating (FBG) arrays can be inscribed in the sensing fibre to increase the signal-to-noise ratio. The interference of the signals reflected by two consecutive FBGs (containing information about the local applied vibration) is subject to a polarization fading effect when the polarization states of the two reflected signals are not aligned. The present work first aims to evaluate by simulation the polarization fading effect in the case of a direct detection phase-OTDR scheme using a standard single mode fibre as the sensing fibre. Then, the simulation tool was extended to estimate the improvement resulting from the use of a spun fibre. Spun fibres can indeed strongly reduce the polarization fading effect in φ-OTDR systems. The next lines present the principle of FBG-assisted Phase-OTDR, followed by a description of the simulation method and a presentation of the results, i.e. the obtained polarization sensitivity for unspun and spun fibres.

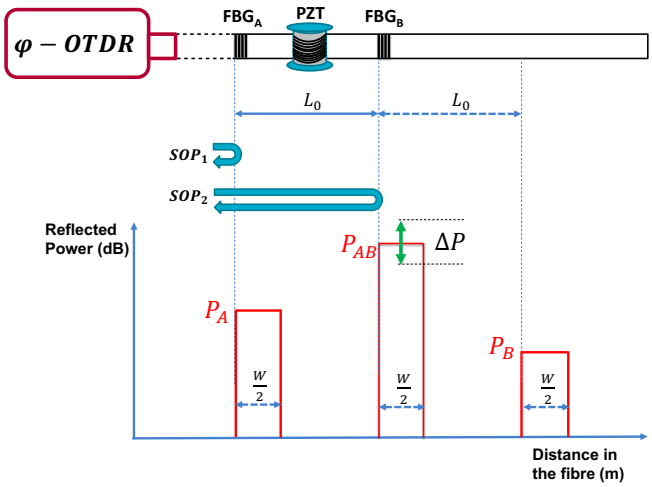

Figure 1: Principle of FBG-assisted Phase-OTDR interrogated by a double pulse signal. For a pair of successive FBGs, the Phase-OTDR trace presents a 3-level feature that includes an interference zone sensitive to the applied vibration.

The principle of FBG-assisted phase-OTDR interrogated with a double pulse is described in figure 1 where two successive weak reflectivity FBGs (FBG_A *and* FBG_B) are written along the sensing fibre. The distance between the FBGs is denoted by L. The coherent laser embedded in the phase-OTDR setup launches two pulses of width W with a delay corresponding in the spatial domain to twice the distance between the FBGs [2]. The phase-OTDR detects the power level P_A (P_B) reflected by FBG_A (FBG_B), and P_{AB}, the interference resulting from the addition of the electric field reflected by FBG_A and FBG_B as [3]:

$$E_{AB} = E_A + E_B \tag{1}$$

$$= \mathrm{E_{in}T^2(t)r_A(t)} + \mathrm{E_{in}[T(t)]^2[t_A(t)]^2r_B(t)e^{j\Delta\phi(t)}d} \tag{1}$$

$$P_{AB} = |E_{AB}|^2 = E_{AB}E_{AB}^* = |E_{in}|^2|T(t)|^4|r_A(t)|^2 + |E_{in}|^2|T(t)|^4|t_A(t)|^4|r_B(t)|^2 \quad (3)$$
$$+2|E_{in}|^2|T(t)|^4|t_A(t)|^2|r_A(t)||r_B(t)|\cos(\Delta\phi(t) + \theta(t)$$

with E_{in} the complex electric field at the FBG array input, $r_A(r_B)$ the complex reflection coefficient of $FBG_A(FBG_B)$, t_A the complex transmission coefficient of FBG_A, $E_A(E_B)$ the electric fields reflected by $FBG_A(FBG_B)$, $\theta(t) = \arg[r_B/r_A]$,and $\Delta\phi(t)$ is twice the phase difference induced between FBG_A and FBG_B. $\Delta\varphi(t)$ varies with time if a vibration is applied thanks to the piezo transducer (PZT). In fact, the PZT, by stretching the fibre between FBGs, allows the variation of optical path difference (OPD) $\Delta L(t)$ and create a phase change of the interference signal [4]. The resulting phase shift $\Delta\phi$(t) is given by $\Delta\phi\ (\mathrm{t}) = \frac{4\pi}{\lambda}\, n\, \Delta L(t)$. Therefore, when a vibration is applied between FBG_A and FBG_B, P_{AB} will vary with time over a ΔP power variation (see figure 1). ΔP depends on the βz product (β is the propagation constant and z the length) integrated over the distance between the successive FBGs. As the Rayleigh backscattering is much smaller than the reflected powers, it can be neglected.

Equation (3) presents the ideal case where the fibre birefringence is not considered. Therefore, the state of polarization SOP_1 and SOP_2 (of the gratings reflected waves) were considered aligned and the ΔP power variation reaches its maximum possible value. When birefringence cannot be neglected, the waves reflected by gratings will be characterized by two different SOPs resulting in a polarization fading coefficient in the P_{AB} expression. When the two SOPs are orthogonal (worst case), the two reflected waves no longer interfere and P_{AB} becomes insensitive to the external perturbation and $\Delta P = 0$. Clearly this situation should be avoided to ensure a good operation of the sensor. The present study analyses the sensitivity of FBG-assisted phase-OTDR systems to polarization fading effect considering unspun and spun fibres. The sensitivity to polarization effects of the sensor can be quantified as the polarization fading sensitivity (PFS) parameter as:

$$PFS = 10\, log_{10}\left(\frac{\Delta P_{max}}{\Delta P_{min}}\right)\ [dB] \quad (4)$$

where $\Delta P_{\max\,(\min)}$ is the maximum (minimum) ΔP observed when sweeping all the possible input SOP (azimuth angle $\varphi \in [0,2\pi]$ and ellipticity angle $\chi \in [-\frac{\pi}{4},\frac{\pi}{4}]$). When SOPs reflected by FBGs are aligned whatever is the input SOP, the PFS is equal to 0 dB ($\Delta P_{max} = \Delta P_{min}$). When the SOPs are orthogonal for at least one of the input SOP, ΔP_{min} = 0 and PFS reaches the infinity. ΔP depends on the input SOP and on the fibre birefringence properties. These two features are therefore taken into account in our modeling. The input SOP (at the input of the first FBG) can be expressed by a Jones vector as given in equation (5):

$$V_n = \begin{pmatrix} V_{nx} \\ V_{ny} \end{pmatrix} = \begin{pmatrix} \cos\varphi\cos\chi - j\sin\varphi\sin\chi \\ j\sin\varphi\sin\chi + j\cos\varphi\sin\chi \end{pmatrix} \quad (5)$$

The birefringence effect of the fibre section between the FBGs is described by the Laming matrix (based on Jones formalism) that relates the input and output SOPs of the fibre section. The Laming matrix allows to model the birefringence effects of both unspun and spun fibres. A spun fibre is a specialty fibre in which the linear birefringence axes (polarization eigenmodes) rotates with a (constant in our case) spin rate ξ (in rad/m).

along the fibre axis in order to reduce the effective global linear birefringence [5]. The specific features of a spun fibre is its spun period $S_P = 2\pi/\xi$ [m] and the local beat length L_B. An unspun fibre corresponds to the case of a linear birefringence medium without polarization mode coupling (the polarization eigenmode are constant along the fibre).

In this work the birefringence of a spun fibre of length z can be described by two lumped birefringent matrix elements: a retarder [Jones matrix R] with principal axis orientation $\varphi(z)$ followed by a rotator matrix $\Omega(z)$. R.I. Laming et al. [5] have presented the Jones matrix describing the fibre by the matrix M. as: $[M] = [\Omega][\mathrm{R}]$ with:

$$[R] = \begin{pmatrix} \cos\frac{R(z)}{2} + \mathrm{j}\sin\frac{R(z)}{2}\cos 2\phi(t) & j\sin\frac{R(z)}{2}\sin 2\phi(z) \\ j\sin\frac{R(z)}{2}\sin 2\phi(t) & \cos\frac{R(z)}{2} - j\sin\frac{R(z)}{2}\cos 2\phi(t) \end{pmatrix} \tag{6}$$

and

$$[\Omega] = \begin{pmatrix} \cos\Omega(z) & -\sin\Omega(z) \\ \sin\ \Omega(z) & \cos\Omega(z) \end{pmatrix} \text{ where } \phi(t) = \frac{\xi z - \Omega(z)}{2} + \frac{m\pi}{2} + \theta_{1s}, \tag{7}$$

$$R(z) = 2\sin^{-1}\left(\frac{1}{(1+q^2)^{1/2}} \cdot \sin\gamma z\right) \text{ and } \Omega(z) = \xi z + \tan^{-1}\left(\frac{-q_L}{(1+q_L^2)^{1/2}}\tan\gamma z\right) \tag{8}$$

with $z = L_0 + \Delta L(t)$, $\Delta L(t)$ is a sinusoidal length variation induced by the vibration frequency and L_0 the initial length of fibre wounded around the PZT. m_L and $n_L$are integers and θ_{1s} is the initial orientation (at $z = 0$) of the local slow axis (the angle between the coordinate system x axis and the slow axis). The parameters q_L and γ_L are defined as followed:

$$q_L = \frac{2(\xi(L_0+\Delta L(t))+f)}{\Delta\beta} \text{ and } \gamma_L = \frac{1}{2}\sqrt{\Delta\beta^2 + 4(\xi+f)^2} \tag{9}$$

where $\Delta\beta$ represents the local linear birefringence (is equal to $2\pi/L_B$). f is the Faraday-induced rotation angle per unit length. f differs from zero when the fibre is subject to a longitudinal magnetic field which is not the case in this work ($f = 0$). For a Laming matrix M in the forward direction, the corresponding Jones matrix in the backward direction is equal to the transpose of M. Therefore, the back and forth propagation in the same fibre is described by the following matrix product: $M_{bf} = M^T M$. The interference power P_{AB} can therefore be recalculated based on the new complex electric field reflected by the gratings:

$$E_A = \begin{pmatrix} E_{Ax} \\ E_{Ay} \end{pmatrix} = r \begin{pmatrix} V_{nx} \\ V_{ny} \end{pmatrix} \tag{10}$$

$$E_B = \begin{pmatrix} E_{Bx} \\ E_{By} \end{pmatrix} = t_A\, M^t\, r_B\, M\, t_A \begin{pmatrix} V_{nx} \\ V_{ny} \end{pmatrix} e^{j\frac{4\pi}{\lambda}n(L_0+\Delta L(t))} \tag{11}$$

$$P_{AB} = |E_{Ax} + E_{Bx}|^2 + |E_{Ay} + E_{By}|^2 \tag{12}$$

where n is the mean refractive index. Figure 2(a) presents the evolution of ΔP while varying in all possible case of input SOPs when $L_B = 4L_0$ (worst case) using an unspun fibre. For some SOP, ΔP is closed to zero so that the PFS reaches 85.24 dB. To mitigate the polarization effect, an example of spun fibre is used with a spun period S_P = 5 m (0.03 m) for a distance between gratings of 40 m and a beat length L_B of 1m. The resulting PFS give 2.21 dB (0.02dB) clearly showing that the use of a spun fibre reduces the PFS and is therefore beneficial for a good operation of the sensor.

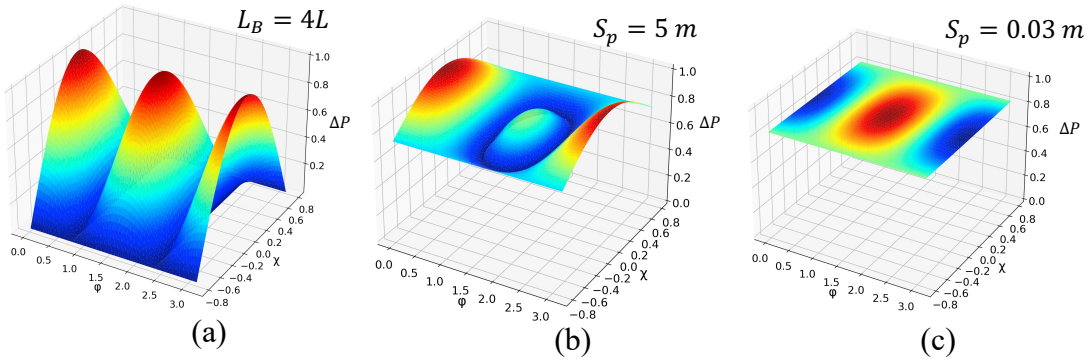

Figure 2: a) $\Delta P\ (\varphi, \xi)$ for a unspun fibre with $L_B = 4L_0$, PFS = 85.24 dB, b) a spun fibre with $S_P = 5m$, PFS = 2.21 dB and c) a spun fibre with $S_P = 0.03\ m$, PFS = 0.02 dB.

Figure 3(a) presents the evolution of PFS as function of L_B/L_0 using an unspun fibre. The high PFS peaks are obtained when $L_B = \frac{4L}{2m+1}$, with m a positive integer. In these case, at least on input SOP results into two nearly orthogonal reflected SOPs. Figure 3(b) presents the PFS evolution as function of L_B/L for different spun period values. The efficiency of spun fibres to mitigate polarisation effect clearly appears (specifically for $S_P < 2m$).

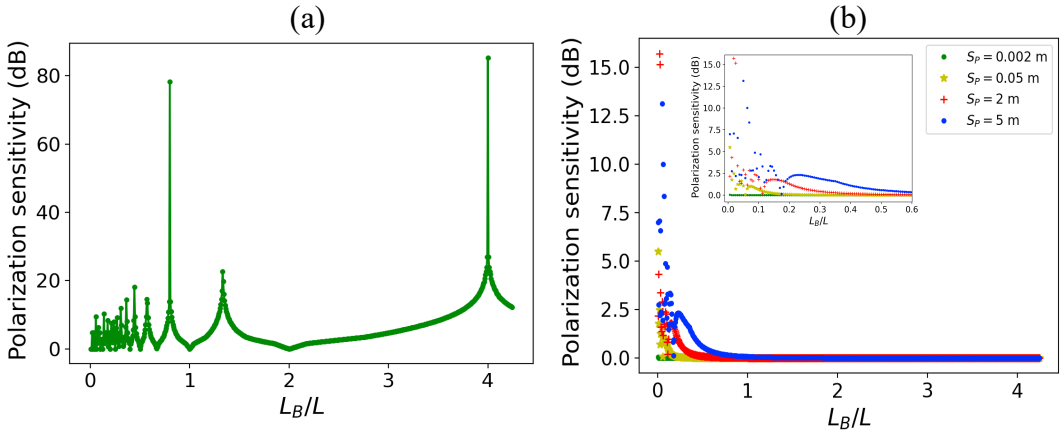

Figure 3: PFS as a function of $\frac{L_B}{L}$ (between 0.25 and 4.25) for $\theta_{1s} = 0$, Λ = 536.42 nm, L_0 = 40m n_0 =1.4471, δn=1.610−5, L_{FBG} = 4 mm, v=1, and Δn =2.

In conclusion, the present study presented a simulation tool that enables to analyse the effect of polarization on a FBG assisted phase-OTDR for both unspun and spun fibres. The spun fibre enables to mitigate the polarisation effects on the system.

[1] M. F. Bado and J. R. Casas, "A Review of Recent Distributed Optical Fiber Sensors Applications for Civil Engineering Structural Health Monitoring," Sensors, vol. 21, no. 5, Art. no. 5, Jan. 2021.

[2] F. Sandah, M. Dossou, and M. Wuilpart, "Spectral Shadowing Compensation in Double-pulse FBG-assisted φ-OTDR," in PIERS 2022, pp. 530–535, 2022.

[3] V. de Miguel Soto et al, "Spectral shadowing suppression technique in phase-OTDR sensing based on weak fiber Bragg grating array," Opt. Lett., vol. 44, no. 3, p. 526, Feb. 2019.

[4] X. Zhang et al., "A high performance distributed optical fiber sensor based on Φ-OTDR for dynamic strain measurement," IEEE Photonics J., pp. 1–1, 2017.

[5] R. I. Laming and D. N. Payne, "Electric current sensors employing spun highly birefringent optical fibers," J. Light. Technol., vol. 7, no. 12, pp. 2084–2094, 1989.